

# Neural Network iLQR: A New Reinforcement Learning Architecture

Zilong Cheng, Jun Ma, Xiaoxue Zhang, Frank L. Lewis, *Life Fellow, IEEE*, and Tong Heng Lee

**Abstract**—As a notable machine learning paradigm, the research efforts in the context of reinforcement learning have certainly progressed leaps and bounds. When compared with reinforcement learning methods with the given system model, the methodology of the reinforcement learning architecture based on the unknown model generally exhibits significantly broader universality and applicability. In this work, a new reinforcement learning architecture is developed and presented without the requirement of any prior knowledge of the system model, which is termed as an approach of a “neural network iterative linear quadratic regulator (NNiLQR)”. Depending solely on measurement data, this method yields a completely new non-parametric routine for the establishment of the optimal policy (without the necessity of system modeling) through iterative refinements of the neural network system. Rather importantly, this approach significantly outperforms the classical iterative linear quadratic regulator (iLQR) method in terms of the given objective function because of the innovative utilization of further exploration in the methodology. As clearly indicated from the results attained in two illustrative examples, these significant merits of the NNiLQR method are demonstrated rather evidently.

**Index Terms**—Reinforcement learning, neural network, trajectory planning, iterative linear quadratic regulator (iLQR), dynamic programming, decision making.

## I. INTRODUCTION

The last decade has witnessed substantial achievements in the context of reinforcement learning [1]–[6]. As one of the machine learning paradigms, reinforcement learning has been widely deployed to solve sequential decision-making problems in various domains, such as robotics, autonomous driving, electronic games, computer vision, healthcare, etc. Basically, the reinforcement learning method can be classified into the model-based method and the model-free counterpart. Particularly, the model-based reinforcement learning method utilizes a predictive model to explore the potential information between the specific objective function and trajectories, such that a satisfying policy can be determined [7], [8]. On the contrary, the model-free reinforcement learning method finds such a policy by exploration, where the model identification procedure is completely bypassed, and only the information

comprising the interaction between the agent and the environment is utilized [9], [10].

It is pertinent to note that the model-based reinforcement learning method has high superiority to utilize the prior knowledge before exploring the environment, which facilitates the search for an optimal policy in many practical applications. Representative model-based reinforcement learning methods include the differential dynamic programming (DDP) [11], [12], iterative linear quadratic regulator (iLQR) [13], [14], and policy search based methods [15], [16]. Apart from the applications where the model-based method is directly used for finding an optimal policy, there exist several practical methodologies that utilize the model-based method to generate the guided searching direction for the model-free reinforcement learning method, such as the Dyna algorithm [17] and the guided policy search method [18], [19]. This combination shows significant improvement in the efficiency of finding a satisfying policy and improving the optimality in terms of the obtained policies. However, for systems with highly complex dynamics (such as the humanoid robot, soft robot, legged robot, unmanned aerial vehicle (UAV), etc.), it generally renders considerable challenges in deriving the system model [20]–[23]. Additionally, the behavior in certain applications is even unmodelable, for example, the electronic game [24]. As a consequence, the model-based reinforcement learning method is no longer effective in such scenarios. Moreover, the policy optimization procedure can sometimes be stuck into a local optimal point due to the high nonlinearity of the dynamic systems.

On the other hand, the existing model-free reinforcement learning method includes the policy-based method [25]–[27], value-based method [28]–[31], and integrated method [32]–[34]. In terms of the policy-based method (such as the policy gradient method), a mapping from the state to the action is explicitly established, and the policy is usually improved after an entire episode. However, the value-based method (such as the deep Q-learning method) aims to construct the mapping among the state, action, and reward. The mapping can be updated immediately after each action, and thus the value-based method is usually more efficient than the policy-based method. After substantial explorations, the mapping to the reward tends to be precise, and the optimal action can be straightforwardly determined in each state. The integrated method [35], [36] (such as the actor-critic method) combines the value-based method and the policy-based method, whereby the merits of both methods are integrated, and thus superior performance usually can be attained in this architecture. Albeit the significant progress related to the development of the

Z. Cheng, X. Zhang, and T. H. Lee are with the NUS Graduate School for Integrative Sciences and Engineering, National University of Singapore, 119077 (e-mail: zilongcheng@u.nus.edu; xiaoxuezhang@u.nus.edu; eleleeth@nus.edu.sg).

J. Ma is with the Department of Mechanical Engineering, University of California, Berkeley, CA 94720 USA (e-mail: jun.ma@berkeley.edu).

F. L. Lewis is with the Automation and Robotics Research Institute, University of Texas at Arlington, Arlington, TX 76118 USA (e-mail: lewis@uta.edu).

This work has been submitted to the IEEE for possible publication. Copyright may be transferred without notice, after which this version may no longer be accessible.

model-free reinforcement learning method, a substantial scale of exploration samples is demanded to reach the satisfying policy.

The contributions of this paper are summarized as follows:

1) A completely new reinforcement learning architecture without the requirement of any prior knowledge of the system model, named the neural network iLQR (NNiLQR), is presented. It solely utilizes the measurement data to facilitate the implementation of the iLQR method and solve the trajectory planning problem based on the neural network.

2) The use of further exploration is presented to prevent the trap from the local optimal point, whereby the optimality of the obtained trajectory can be further improved. Thus with the same setting of the initial feasible trajectory, the NNiLQR approach can even find a better trajectory as compared to the one obtained by the classical iLQR method.

3) With this data-driven framework, it is shown how the perturbed gradient information can be extracted from the data such that it can be successfully adopted to improve the current trajectory.

4) The proposed NNiLQR method is validated through extensive simulations on vehicle tracking and cartpole swing-up examples. It is also shown how the NNiLQR method is influenced by critical factors such as the neural network structure and etc.

## II. RELATED WORK

Several related works have been conducted in the past few years. Regarding the utilization of the similar framework for the implementation of the DDP and iLQR methods, the earliest work we can find is [37], in which a locally weighted projection regression (LWPR) method is utilized to complete the non-parametric model identification, and then the iLQR method is performed as a feedforward controller to realize the objective of tracking. Moreover, [38] utilizes the iLQR method to guide the policy search direction in the reinforcement learning method. In [38], both the model-based and model-free architectures are discussed. Besides, in [39], a Bayesian non-parametric representation of the unknown dynamics is utilized to deploy the DDP method. After that, [40] proposes the use of the temporally decomposed dynamics to improve the performance of the DDP framework, where a locally weighted regression method is applied to fit the whole system dynamics. Furthermore, the authors utilize the neural network to fit the temporally decomposed dynamics to further improve the architecture in [41]. In [42], the authors propose using two neural networks to employ the iLQR method, where one neural network called the torque neural network focuses on mapping the system state to the action sequences; meanwhile, the other one is used to realize the feedback pass in the iLQR method. Besides the works as mentioned above, several closely related works are developed very recently. In [43], an iLQR framework called the curious iLQR is proposed, in which the system dynamics is reflected by the Bayesian modeling. [44] proposes the use of a neural network to model the dynamics of off-road and on-road vehicles, and real-world experimental results are provided. [45] proposes a structured

linear parameterization method of a feedback policy, and then the iLQR method is subsequently realized in a sample-efficient manner.

Apart from the most related works, some other similar pertinent results are also achieved to solve similar problems based on the DDP and iLQR methods in the reinforcement learning fields. [46] presents an online trajectory optimization method based on the iLQR scheme for highly complex systems. In [47], the authors present a trajectory optimization approach in terms of the continuous state and action spaces based on the probabilistic DDP, in which the prior model knowledge can be incorporated to promote the learning process.

These works prominently show the high applicability of the iLQR scheme. Notably, these works are certainly not only restricted to trajectory optimization but also can be generalized in broad applications of reinforcement learning.

## III. NEURAL NETWORK iLQR

In this section, the NNiLQR approach is presented with a detailed analysis. Significantly distinct from the Deep Q-Networks (DQN) method that employs a deep neural network to map pairs of states and actions to the corresponding reward values, the NNiLQR method utilizes the neural network to learn the dynamic function. With the proposed development, the classical iLQR method can be performed entirely based on the measurement data with the incorporation of the neural network.

### A. Preliminary

Generally, with the terminal objective function considered, an optimization problem for the DDP and iLQR methods can be formulated as a nonlinear non-convex optimization problem, which can be expressed as

$$\begin{aligned}
 & \underset{(x(\tau), u(\tau)) \in \mathbb{R}^n \times \mathbb{R}^m}{\text{minimize}} && J_T(x(T)) + \sum_{\tau=0}^{T-1} J_\tau(x(\tau), u(\tau)) \\
 & \text{subject to} && x(\tau + 1) = f(x(\tau), u(\tau)) \\
 & && \tau = 0, 1, \dots, T - 1 \\
 & && x(0) = x_0,
 \end{aligned} \tag{1}$$

where  $x(\tau) \in \mathbb{R}^n$  and  $u(\tau) \in \mathbb{R}^m$  denote the state and action in the Markov Decision Processes (MDP) at the time stamp  $\tau$ , respectively;  $J_\tau(x(\tau), u(\tau))$  denotes the reward at each time stamp  $\tau$  with respect to the pair of state and action;  $f(x(\tau), u(\tau))$  is the dynamic function of the system;  $x_0$  denotes the initial state of the system. Notably, the objective function, which is defined as the summation of all rewards, can be chosen in any smooth type such as linear quadratic function, Huber Function, and log barrier function, and it is pertinent to note that the dynamic function  $f$  is not restricted to be linear.

The principle idea of the DDP and iLQR methods generalizes from the dynamic programming, which can be straightforwardly represented by the Bellman equation given by

$$V_\tau(x(\tau)) = \min_{u(\tau)} \left\{ J_\tau(x(\tau), u(\tau)) + V_{\tau+1}(f(x(\tau), u(\tau))) \right\}, \tag{2}$$

where  $V_\tau(x(\tau))$  and  $V_{\tau+1}(f(x(\tau), u(\tau)))$  denote the value functions with respect to the current state  $x(\tau)$  and the state at the next time stamp  $x(\tau + 1)$ , respectively.

Before the DDP and iLQR methods are realized, a feasible nominal trajectory  $\{\hat{u}(\tau), \hat{x}(\tau)\}_{\tau=0}^T$  is pre-defined. To generate such a feasible nominal trajectory, we can determine an initial state and choose a sequence of nominal actions. After the initial trajectory is generated, the so-called backward pass of the DDP and iLQR methods can be performed. The iteration starts with the value function at the last time stamp, i.e.,  $V_T(x(T)) = \phi(x(T))$ , and proceeds backwards until the value function at the first time stamp is involved.

To realize the backward pass, the perturbed Q-function is introduced and denoted by  $Q_\tau(\delta x(\tau), \delta u(\tau))$ , where  $\delta x(\tau)$  and  $\delta u(\tau)$  represent the amount of change with respect to the state and action at the time stamp  $\tau$ , respectively. Then with the Bellman equation (2), we can express the perturbed Q-function as

$$\begin{aligned} & Q_\tau(\delta x(\tau), \delta u(\tau)) \\ &= J_\tau(x(\tau) + \delta x(\tau), u(\tau) + \delta u(\tau)) - J_\tau(x(\tau), u(\tau)) \\ &+ V_{\tau+1}(f(x(\tau) + \delta x(\tau), u(\tau) + \delta u(\tau))) \\ &- V_{\tau+1}(f(x(\tau), u(\tau))). \end{aligned} \quad (3)$$

Notably, in the method of DDP, the perturbed Q-function is approximated by the second-order Taylor expansion, and then it can be compactly denoted by the following matrix equation:

$$\begin{aligned} & Q_\tau(\delta x(\tau), \delta u(\tau)) \\ &\approx \frac{1}{2} \begin{bmatrix} 1 \\ \delta x(\tau) \\ \delta u(\tau) \end{bmatrix}^T \begin{bmatrix} 0 & (Q_\tau^T)_x & (Q_\tau^T)_u \\ (Q_\tau)_x & (Q_\tau)_{xx} & (Q_\tau)_{xu} \\ (Q_\tau)_u & (Q_\tau)_{ux} & (Q_\tau)_{uu} \end{bmatrix} \begin{bmatrix} 1 \\ \delta x(\tau) \\ \delta u(\tau) \end{bmatrix}, \end{aligned} \quad (4)$$

where the subscript of each matrix function denotes the first-order and second-order derivative with respect to the corresponding variable. Hence, the derivative of these matrices can be explicitly obtained by

$$\begin{aligned} (Q_\tau)_x &= (J_\tau)_x + f_x^T(V_{\tau+1})_x \\ (Q_\tau)_u &= (J_\tau)_u + f_u^T(V_{\tau+1})_u \\ (Q_\tau)_{xx} &= (J_\tau)_{xx} + f_x^T(V_{\tau+1})_{xx}f_x + (V_{\tau+1})_x \cdot f_{xx} \\ (Q_\tau)_{ux} &= (J_\tau)_{ux} + f_u^T(V_{\tau+1})_{xx}f_x + (V_{\tau+1})_x \cdot f_{ux} \\ (Q_\tau)_{uu} &= (J_\tau)_{uu} + f_u^T(V_{\tau+1})_{xx}f_u + (V_{\tau+1})_x \cdot f_{uu}, \end{aligned} \quad (5)$$

where the operator  $(\cdot)$  in the last three sub-equations denotes the contraction operation between a vector and a tensor.

In terms of the perturbed Q-function, the optimal solution to the perturbed control action  $\delta u(\tau)^*$  at the time stamp  $\tau$  is represented by

$$\delta u(\tau)^* = \operatorname{argmin}_{\delta u(\tau)} Q_\tau(\delta x(\tau), \delta u(\tau)). \quad (6)$$

Then, to further complete the backward iterations numerically, we can reformulate the the optimal perturbed control action in terms of the perturbed Q-function as a linear form, which is given by

$$\delta u(\tau)^* = k(\tau) + K(\tau)\delta x(\tau), \quad (7)$$

where  $k(\tau) \in \mathbb{R}^m$  and  $K(\tau) \in \mathbb{R}^{m \times n}$  are the feedforward vector and feedback gain matrix for the perturbed Q-function at the time stamp  $\tau$ , respectively, and they can be explicitly represented by

$$k(\tau) = -(Q_\tau)_{uu}^{-1} (Q_\tau)_u \quad (8a)$$

$$K(\tau) = -(Q_\tau)_{uu}^{-1} (Q_\tau)_{ux}. \quad (8b)$$

Then the gradient and Hessian of the value function at each time stamp can be obtained by substituting (8a) and (8b) to the Taylor expansion of perturbed Q-function, and it follows that

$$(V_\tau)_x = (Q_\tau)_x - K(\tau)^T (Q_\tau)_{uu} k(\tau) \quad (8c)$$

$$(V_\tau)_{xx} = (Q_\tau)_{xx} - K(\tau)^T (Q_\tau)_{uu} K(\tau). \quad (8d)$$

Assuming the value function after the last time stamp is zero, then we can complete the backward pass by recursively calculating (5), (8a), (8b), (8c), and (8d) from the last time stamp to the first time stamp. It is noteworthy to mention that the iLQR method is a variant of the DDP method, and the main difference is that the DDP method involves the Hessian matrix of the system dynamic function, while the Hessian matrix is neglected in the iLQR method. Note that since the existing works in the literature demonstrates higher performance of the iLQR method compared to the DDP method, in the following analysis, only the iLQR method will be discussed.

Then, after the backward pass, the so-called forward pass is carried out subsequently. In the forward pass, the trajectory of the system is generated by using the system dynamic function and the sequence of actions pre-determined in the backward pass. With the system dynamic function in (1), perturbed control actions (7), feedforward vector (8a), and feedback matrix (8b), we have

$$\begin{aligned} u(\tau) &= \hat{u}(\tau) + k(\tau) + K(\tau)(x(\tau) - \hat{x}(\tau)) \\ x(\tau + 1) &= f(x(\tau), u(\tau)). \end{aligned} \quad (9)$$

After the backward pass is done, one iLQR iteration is completed. Then the nominal trajectory  $(\hat{x}, \hat{u})$  can be updated to a new feasible trajectory obtained in the forward pass, and the updated feasible trajectory can be used to initiate the next iLQR iteration. After several iterations, the trajectory will converge asymptotically, and the objective function will be reduced to a sub-optimal point. Notably, a line search procedure is usually included because the convergence cannot be guaranteed in the general cases with the classical iLQR method. The iLQR method with the line search strategy are summarized in Algorithm 1.

## B. Impediments to the Realization

The first impediment is the unlimited range of the state variables and action variables. To be more specific, some of the state variables and action variables are generally not bounded in most practical applications (for example, the position state of a vehicle model can certainly be infinite). In the context of learning methods, they render great difficulties predicting the data that is out of the range of the training set, and thus it is rather onerous to use the existing learning methods to predict

---

**Algorithm 1** iLQR Algorithm with Line Search

---

**Require:** Prediction Horizon  $T$ ;  
Objective function  $J_\tau$  and system dynamic function  $f$ ;  
The maximum number of line search iterations  $\ell_{\max}$ ;  
The maximum number of iLQR iterations  $i_{\max}$ .

- 1: **Step 1: (Initialization)**
- 2: Choose the initial feasible nominal trajectory  $(\hat{x}(\tau), \hat{u}(\tau))$ .
  
- 3: Set  $(V_{T+1})_x = 0, (V_{T+1})_u = 0, (V_{T+1})_{xx} = 0$ .
- 4: **for**  $i = 0, 1, \dots, i_{\max}$  **do**
- 5:   **Step 2: (Backward Pass)**
- 6:   **for**  $\tau = T, T-1, \dots, 0$  **do**
- 7:     Derive vectors  $(Q_\tau)_x, (Q_\tau)_u$  and matrices  $(Q_\tau)_{xx}, (Q_\tau)_{ux}, (Q_\tau)_{uu}$  by (5).
- 8:     Derive the vector  $k(\tau)$  and matrix  $K(\tau)$  by (8a) and (8b).
- 9:     Derive the vector  $(V_\tau)_x$  and matrix  $(V_\tau)_{xx}$  by (8c) and (8d).
- 10:   **end for**
- 11:   **Step 3: (Forward Pass)**
- 12:   **for**  $k = 0, 1, \dots, \ell_{\max}$  **do**
- 13:     **for**  $\tau = 0, 1, \dots, T$  **do**
- 14:       Generate the new trajectory  $(\hat{x}(\tau), \hat{u}(\tau))$  by (9).
- 15:     **end for**
- 16:     Do line search.
- 17:   **end for**
- 18:   **if** stopping criterion is satisfied **then**
- 19:     **return** current trajectory  $(\hat{x}(\tau), \hat{u}(\tau))$ .
- 20:   **else**
- 21:     Update the nominal trajectory.
- 22:   **end if**
- 23: **end for**

---

the full dynamics of a system. Admittedly, the same challenge inevitably exists in the NNiLQR method.

Secondly, it is challenging to use a neural network to learn a dynamic system with high dimensions. In these cases, it is usually cumbersome to gather the measurement data and complete the data pre-processing because of the large dimensions. However, it is acknowledged that a neural network with a large size is preferred in these circumstances, because a neural network with a small size cannot fit the system dynamics very well (due to the insufficient number of parameters). Essentially, a large-scale neural network requires a dataset with a considerable size to complete the training process, and thus it leads to an insoluble dilemma between the choice of the network scale and dataset size.

Thirdly, the notably high nonlinearity in complex systems brings new challenges to the existing learning methods. Due to the limited time of exploration in the experiment of dynamic systems, it is clearly impossible to visit each pair of the state and action. Hence, after the training process, the neural network cannot sufficiently and accurately map the nonlinearity of the target system based on a limited number of exploration. The learning model's inaccuracy can certainly lead to a vital difference between the given decision and the optimal decision in terms of the dynamic system.

Finally, throughout the implementation of the iLQR method, the gradient of the dynamic function is required. As discussed above, there exists a significant difference between the dynamic system and the trained neural network. In this situation, the gradient of the neural network model contains a large amount of noises and ineffective information. Thus, it is also a challenge to extract the valuable information from the perturbed derivative information.

In the following text, we will show how these impediments can be effectively addressed by our development here.

### C. Setup

Fig. 1 shows the workflow of how the NNiLQR method is implemented. Basically, in each iteration, there exist three steps during the application of the NNiLQR method. At the beginning of the NNiLQR method, an empty dataset is required to be initialized with a given size of  $p \times T$ , where  $p$  denotes the number of trials and  $T$  denotes the prediction horizon. After the initialization,  $p$  random trials are necessary to be performed in the dynamic system (i.e., the system runs arbitrarily with a sequence of actions chosen randomly). The initial state of each trial is supposed to be the same, and the sequence of actions in each trial can be extracted from a designated probabilistic distribution (e.g., normal distribution, uniform distribution). This initialization procedure for the dynamic system is the so-called initial exploration period. Even though the sequence of actions can be generated under a specific probabilistic distribution, an evaluation procedure can be employed to avoid ineffective actions during the exploration. In other words, we can remove the inappropriate data from the dataset before training the neural network. For instance, in terms of the vehicle tracking problem, if a group of data shows that the vehicle goes in the opposite direction, we can directly eliminate this group of data from the dataset because it absolutely does not make any contribution to the neural network training. Though the evaluation procedure is optional, it can significantly shorten the time for finding a feasible trajectory.

There are several ways to complete the evaluation task. For example, one more neural network can be utilized to judge whether the current data is valuable. Besides, intuitive methods such as setting thresholds for particular state variables are also usually practically realistic. Moreover, the intuitive choice of the range of action variables is fairly preferred. For example, suppose there are two action variables in the vehicle tracking problem, i.e., the steering angle  $\theta$  and the acceleration  $a$ , and a uniform distribution is used to generalize the sequence of actions. If the target position of the vehicle is in the positive direction of its initial position, we can set the steering angle to be limited within a small range (such that the vehicle will not perform a U-turn during the initial exploration period), and also, we can set a positive range of the acceleration (such that the vehicle will not perform reversing)

Notably, in some practical cases, a maximum number of NNiLQR iterations must be chosen because it is not straightforward to determine the stopping criterion. This strategy is not strange in the field of learning, as under certain scenarios,

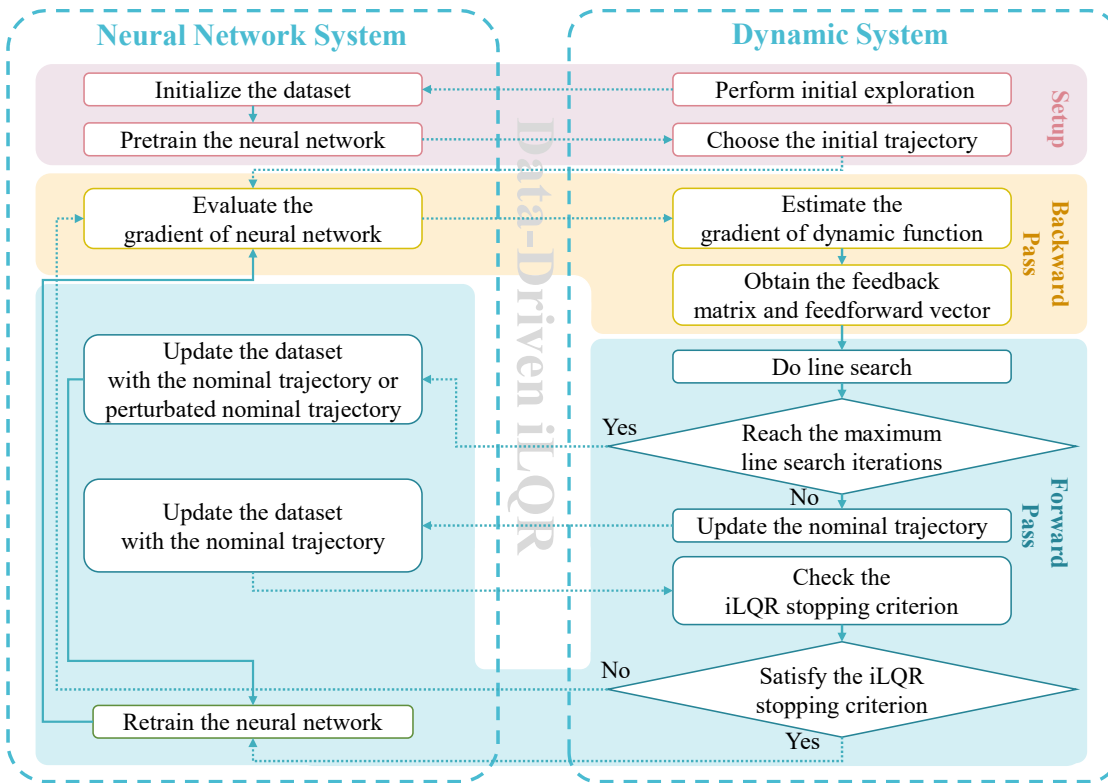


Fig. 1. Flow chart of the neural network iterative linear quadratic regulator.

the global optimum is not exactly known. Taking the cartpole as an example, we may successfully swing up the cartpole system after several trials using the proposed reinforcement learning method. However, from the viewpoint of the objective function, the successful swing-up indeed does not provide a satisfying objective function value. Then in this situation, the choice of the maximum number of trials is absolutely essential.

Upon completion of the dataset initialization, a neural network structure can be chosen to fit the system dynamic function. A variety of neural networks are suitable for fitting the dynamic function, and we will compare the performance of several widely used neural network structures in Section IV and Section V-A in detail. Given the optimization algorithm, the chosen neural network can be pretrained based on the initial dataset. Remarkably, since it is highly time-consuming to perform the initial exploration period, the number of the initial trials is usually chosen in a moderate size, such as 100 trials. Apparently, after pretraining, the neural network still renders difficulty in fitting the dynamic function precisely due to the aforementioned impediments, and thus it is impossible to use the pretrained neural network in the iLQR iteration directly. From the authors' experience, under no circumstances the direct use of the pretrained network can provide a satisfying result.

#### D. Backward Pass

Similar to the classical DDP and iLQR method, an initial nominal feasible trajectory is required before the first backward pass is performed. Therefore, the methods for initial

trajectory selection deployed in the classical DDP and iLQR frameworks can be directly borrowed to facilitate the development of the NNiLQR method. For example, we can set all actions to be zero or use the imitation learning data. Then, after the initial trajectory is obtained, the gradient of the neural network with respect to each pair of the state and action can be calculated. It is worthwhile to mention that there are several methods available in the literature for deriving the gradient. For instance, the automatic differentiation method based on the chain rule is the most straightforward option to be utilized as it has been integrated into many existing solvers. Besides, for those neural networks with a simple network structure, it is possible to derive the gradient with the analytical method. In the NNiLQR method, it can be much more efficient if the analytical method is implemented. This is because once the neural network structure is fixed, the analytical gradient of the neural network is also fixed. Subsequently, in each iLQR iteration, the gradient can be directly obtained by some simple algebraic computations. Additionally, the numerical method is also one of the possible choices of gradient computation.

Note that the gradient of the neural network could greatly differ from the gradient of the system dynamic function. This is because the size of the dataset can be chosen as a very small number in the NNiLQR method. Moreover, a small disturbance in the neural network parameters can cause a significant change in the neural network gradient matrix, which also substantially results in the inaccuracy in the gradient matrix. Thus, it is essential to include some polishing approaches to estimate the value of the gradient matrix of the system

dynamic function. Here, we introduce a feasible solution in view of continuity. It is pertinent to mention that the gradient of the dynamic function  $f$  is continuous in the majority of motion planning problems, and thus the matrix functions  $f_x$  and  $f_u$  are continuous matrix functions. We denote the neural network that fits the system dynamic function  $f$  by  $\mathcal{N}$ . Then we have the mapping between the state and action at the time stamp  $\tau$  and the state at the time stamp  $\tau + 1$ , which can be represented by  $x(\tau + 1) = \mathcal{N}(x(\tau), u(\tau))$ .

Obviously, it is impossible to ensure the continuity of the gradient of the neural network  $\mathcal{N}_x$  and  $\mathcal{N}_u$  because of the existence of the non-smooth functions in the neural network, even if in the case where the neural network  $\mathcal{N}$  can fit the system dynamic function  $f$  very well. Therefore, in the NNiLQR method, we propose the use of filters to enhance continuity. For example, one typical choice could be a one dimension truncated Gaussian filter. The detailed discussion on the influence of the Gaussian filter will be given in Section V-B. Finally, when the gradient of the system dynamic function is derived, the backward pass can be carried out in the same manner as the classical DDP and iLQR methods. After the completion of the backward pass, a feedback matrix and a feedforward vector is generated for each time stamp. Notably, The information of the objective function with the second-order Taylor expansion and the dynamic function with the first-order Taylor expansion, with respect to the nominal trajectory, is completely included in the feedback matrices and feedforward vectors. Particularly, the following optimization problem is introduced:

$$\begin{aligned} & \underset{(\delta x(\tau), \delta u(\tau)) \in \mathbb{R}^n \times \mathbb{R}^m}{\text{minimize}} \\ & \frac{1}{2} \sum_{\tau=0}^{T-1} \left( \begin{bmatrix} \delta x(\tau) \\ \delta u(\tau) \end{bmatrix}^T Q_\tau \begin{bmatrix} \delta x(\tau) \\ \delta u(\tau) \end{bmatrix} + \begin{bmatrix} \delta x(\tau) \\ \delta u(\tau) \end{bmatrix}^T q_\tau \right) \\ & \text{subject to } \delta x(\tau + 1) = F_\tau \begin{bmatrix} \delta x(\tau) \\ \delta u(\tau) \end{bmatrix}, \\ & \quad \forall \tau = 0, 1, \dots, T - 1 \\ & \quad \delta x(0) = 0, \end{aligned} \quad (10)$$

where given a nominal trajectory, the matrix  $Q_\tau$  and the vector  $q_\tau$  are the parameter matrix and vector for the objective function with the second-order Taylor expansion at the time stamp  $\tau$ ; the matrix  $F_\tau$  is the system dynamic function with the first-order Taylor expansion in terms of the given trajectory;  $\delta x(0)$  is the perturbed state at the first time stamp given by zero as we assume the initial state remains unchanged when the NNiLQR method is implemented. In fact, given a controller with a linear structure, the optimization problem (10) can be solved globally. Indeed, the optimization problem (10) is a convex optimization problem, where the objective function is with the linear quadratic form and all the invoked equality constraints are affine. If we fix the controller structure with

$$\delta u(\tau) = k(\tau) + K(\tau)\delta x(\tau), \quad (11)$$

then given any nominal trajectory, the backward pass provides the globally optimal solution to the optimization problem (10), and this solution is completely reflected in the feedback matrix  $K(\tau)$  and the feedforward vector  $k(\tau)$  in each time stamp.

### E. Forward Pass

The last and the principal step in the NNiLQR method is the forward pass. An indispensable line search strategy is performed at the beginning of the forward pass to find a trajectory with better performance based on the given feedback matrices and feedforward vectors. Then the basic idea of the line search can be realized by

$$\delta u(\tau) = \alpha k(\tau) + K(\tau)\delta x(\tau), \quad (12)$$

where  $\alpha$  is the step size parameter to be determined in the line search iteration.

The primary goal of the line search method is to ensure the performance of the trajectory can be improved after each iteration, and even if, in the worst case, the line search method guarantees that the trajectory during NNiLQR iterations will not diverge. On the basis of this principle, the most fundamental line search methods work well in the NNiLQR method. For example, in each line search iteration, the current objective function value is compared to the best objective function value before the current iteration. If the performance of the current trajectory is better, then the nominal trajectory can be updated as the current trajectory. On the contrary, if the performance of the current trajectory is worse, then the step size  $\alpha$  is updated to be a smaller value, and the subsequent line search iteration is performed until the maximum number of line search iterations is reached.

In the case where the maximum number of line search iterations is not reached, we can update the dataset with the nominal trajectory, which means the trajectory of the earliest trial in the dataset is replaced by the current nominal trajectory. This step ensures that the dataset contains the trajectory with the current best performance. Remarkably, even though the dataset is updated, the neural network system is not retrained in the current forward pass step.

Next, we can check the stopping criterion for the whole NNiLQR iterations. If the stopping criterion is satisfied, then one NNiLQR iteration is considered completed, and the neural network system will be retrained based on the updated dataset. The next NNiLQR iteration will start from the backward pass of the neural network system. If not, the backward pass in the neural network system will be performed again without retraining the neural network. The stopping criterion is also flexible to be determined. In most general cases, the stopping criterion can be chosen as the difference of the objective function value between the current nominal trajectory and the latest nominal trajectory.

It is vitally important to consider the case when the maximum number of line search iterations is reached. Because it is admitted that there exists a significant difference between the neural network system and the dynamic system. Even though the estimated gradient of the dynamic function is polished before it is utilized, there exists a situation where the corresponding feedback matrices and feedforward vectors are not able to provide an appropriate direction to improve the dynamic system performance further. That means, even if with the smallest step size, it is still not possible to improve the dynamic system performance at all. In this scenario, the

maximum number of line search iterations will definitely be reached. Indeed, through the simulation, it shows that this situation could happen rather frequently when the trajectory approaches the optimal point. Hence, the extent to which the system performance can be further improved when the trajectory is nearly optimal is mainly dependent on how to handle this situation.

In this paper, we propose the use of further exploration to handle this situation. There are two possible situations when the maximum number of line search iterations is reached. The first situation is that the maximum number of line search iterations is reached after several backward and forward passes in the current NNiLQR iteration. In this case, only the nominal trajectory is updated because the feedback matrix  $K$  and feedforward vector  $k$  indeed provide an appropriate direction. The other situation is that only one backward pass and one forward pass are performed in the current NNiLQR iteration, and then the maximum number of line search iterations is reached. In this case, the feedback matrix  $K$  and feedforward vector  $k$  do not provide any useful direction to improve the performance further, and thus the dynamic system will try to further explore the environment based on the current best trajectory. Therefore, in the latter situation, we add some perturbations to the sequence of actions in the current best trajectory, then we generate a new trajectory based on the new sequence of actions, which is the so-called the perturbed nominal trajectory. Subsequently, we update the dataset with the perturbed nominal trajectory and retrain the neural network based on the updated dataset.

It is also noteworthy to mention that the stopping criterion for the retraining is also flexible to be set. An intuitive strategy for choosing the retraining stopping criterion is that the stopping criterion in terms of the training loss is set to be linearly decreased because further exploration will increase the similarity of data in the training set, which will lead to the smaller training loss. However, the stopping criterion cannot be set too small to terminate the retraining, and thus, a lower bound value of the stopping criterion is also necessary to be given.

To this point, the whole picture of the NNiLQR has been introduced. For the sake of clarity, the detailed implementation of the NNiLQR method is summarized in Algorithm 2.

#### IV. ILLUSTRATIVE EXAMPLES AND NEURAL NETWORKS

In this section, two examples are presented to demonstrate the performance of the NNiLQR method. The first example is related to the on-road autonomous driving task, and the second example is on control of a cartpole system.

##### A. Problem Formulation

1) *Vehicle Tracking Example:* The state vector of the vehicle dynamic function is defined as  $x = [p_x \ p_y \ \theta \ v]^T$ , where  $p_x$  and  $p_y$  denote the position of the center of the rear axis in the Cartesian coordinates;  $\theta$  denotes the heading angle of the vehicle;  $v$  denotes the velocity of the vehicle. The action vector of the vehicle system is defined as  $u = [\omega \ a]^T$ , where  $\omega$  denotes the steering angle and  $a$  denotes the acceleration.

---

#### Algorithm 2 Neural Network iLQR Algorithm

---

**Require:** Prediction horizon  $T$ ;  
The maximum number of line search iterations  $\ell_{\max}$ ;  
The maximum number of NNiLQR iterations  $i_{\max}$ ;  
Number of initial trials  $p$ ;  
Initial feasible nominal trajectory  $(\hat{x}(\tau), \hat{u}(\tau))$ ;  
Objective function  $J_\tau$  and system dynamic function  $f$ .

- 1: **Step 1: (Setup)**
- 2: Perform initial exploration and initialize the dataset.
- 3: Choose the neural network structure and pretrain the neural network.
- 4: Choose the initial feasible nominal trajectory  $(\hat{x}(\tau), \hat{u}(\tau))$ .
- 5: Set  $(V_{T+1})_x = 0$ ,  $(V_{T+1})_u = 0$ ,  $(V_{T+1})_{xx} = 0$  for the dynamic system.
- 6: **for**  $i = 0, 1, \dots, i_{\max}$  **do**
- 7:   **Step 2: (Backward Pass)**
- 8:   **for**  $\tau = T, T-1, \dots, 0$  **do**
- 9:     (Neural network system) Derive matrices  $f_x$  and  $f_u$ .
- 10:     (Dynamic system) Polish matrices  $f_x$  and  $f_u$ .
- 11:     (Dynamic system) Derive vectors  $(Q_\tau)_x$ ,  $(Q_\tau)_u$  and matrices  $(Q_\tau)_{xx}$ ,  $(Q_\tau)_{ux}$ ,  $(Q_\tau)_{uu}$  by (5).
- 12:     (Dynamic system) Derive the vector  $k(\tau)$  and matrix  $K(\tau)$  by (8a) and (8b).
- 13:     (Dynamic system) Derive the vector  $(V_\tau)_x$  and matrix  $(V_\tau)_{xx}$  by (8c) and (8d).
- 14:   **end for**
- 15:   **Step 3: (Forward Pass)**
- 16:   **for**  $k = 0, 1, \dots, \ell_{\max}$  **do**
- 17:     **for**  $\tau = 0, 1, \dots, T$  **do**
- 18:       (Dynamic system) Generate the new trajectory  $(\hat{x}(\tau), \hat{u}(\tau))$  by (9).
- 19:     **end for**
- 20:     Do line search.
- 21:     **if** line search requirement is satisfied **then**
- 22:       (Dynamic system) Update the nominal trajectory.
- 23:       (Neural network system) Update the dataset.
- 24:       **if** stopping criterion is satisfied **then**
- 25:         (Neural network system) Retrain the neural network on the updated dataset.
- 26:       **end if**
- 27:       Update the NNiLQR iteration index  $i = i + 1$ .
- 28:       **go to** Step 2.
- 29:     **end if**
- 30:   **end for**
- 31:   (The maximum number of line search iterations is reached)
- 32:   **if** nominal trajectory is updated in the current NNiLQR iteration **then**
- 33:     Update the dataset with the nominal trajectory.
- 34:   **else**
- 35:     Update the dataset with the perturbed nominal trajectory.
- 36:   **end if**
- 37:   Retrain the neural network on the updated dataset.
- 38: **end for**
- 39: **return** Current trajectory  $(\hat{x}(\tau), \hat{u}(\tau))$ .

---

Given the sampling time  $h$ , the rolling distance in terms of the front wheels is given by

$$\mathcal{F}(v) = hv, \quad (13)$$

and the rolling distance in terms of the rear wheels can be represented by

$$\mathcal{R}(v, \omega) = d + \mathcal{F}(v) \cos(\omega) - \sqrt{d^2 - \mathcal{F}(v)^2 \sin^2(\omega)}, \quad (14)$$

where  $d$  denotes the distance between the front axle and the rear axle. The dynamic function of the vehicle can be represented by

$$\begin{aligned} p_x(\tau + 1) &= p_x(\tau) + \mathcal{R}(v(\tau), \omega(\tau)) \cos(\theta(\tau)) \\ p_y(\tau + 1) &= p_y(\tau) + \mathcal{R}(v(\tau), \omega(\tau)) \sin(\theta(\tau)) \\ \theta(\tau + 1) &= \theta(\tau) + \sin^{-1} \left( \frac{\mathcal{F}(v)}{d} \sin(\omega(\tau)) \right) \\ v(\tau + 1) &= v(\tau) + ha(\tau). \end{aligned} \quad (15)$$

In this paper, the parameters in the vehicle example are given as follows. The sampling time is chosen as  $h = 0.1$  and the distance  $d$  is given by  $d = 3$ . The objective function is chosen as a typical linear quadratic form with constant weighting matrices  $Q$  and  $R$  and constant reference trajectory  $r$ :

$$J = \sum_{\tau=0}^T \left( (x(\tau) - r)^T Q (x(\tau) - r) + u(\tau)^T R u(\tau) \right), \quad (16)$$

where the reference trajectory is chosen as  $r = [0 \ -10 \ 0 \ 8]^T$ ; the weighting matrices are chosen as  $Q = \text{diag}\{0, 1, 1, 1\}$  and  $R = \text{diag}\{10, 10\}$ . Based on the given objective function, the vehicle should track the reference  $p_y = -10$  with the velocity  $v = 8$  and the heading angle  $\theta = 0$ . The initial state vector is chosen as  $x_0 = [0 \ 0 \ 0 \ 0]^T$ , which means that initially, the static vehicle parks at the original point with zero heading angle.

The pretraining details are given as follows. The number of trials is chosen as 100, and the prediction horizon is chosen as 100. The initial states are all chosen as zero at the time stamp  $\tau = 0$ . The steering angle  $\omega$  is drawn from a uniform distribution within the range  $[-1, 1]$ . The acceleration  $a$  is drawn from a uniform distribution within the range  $[0, 10]$ .

2) *Cartpole Swing-up Example*: The state vector of the cartpole dynamic function is defined as  $x = [\theta \ \omega \ p \ v]^T$ , where  $\theta$  and  $\omega$  denote the angle between the pole and the vertical direction and its corresponding angular velocity, respectively;  $p$  and  $v$  denote the position and the velocity of the cart, respectively. The action variable of the cartpole system is denoted by  $F$ , which means the force applied to the cart. The gravitational acceleration, sampling time, mass of the cart, mass of the pole, and half length of the pole are denoted by  $g, h, m_c, m_p, \ell$ , respectively. Further define the angular acceleration as  $\alpha$  and the acceleration of the cart as  $a$ :

$$\begin{aligned} \alpha(\theta, \omega, F) &= \frac{g \sin(\theta) + \cos(\theta) \left( \frac{-F - m_p \ell \omega^2 \sin(\theta)}{m_c + m_p} \right)}{\ell \left( \frac{4}{3} - \frac{m_p \cos^2(\theta)}{m_c + m_p} \right)} \\ a(\theta, \omega, F) &= \frac{F + m_p \ell (\omega^2 \sin(\theta) - \alpha \cos(\theta))}{m_c + m_p}. \end{aligned} \quad (17)$$

It follows that the cartpole model can be represented by

$$\begin{aligned} \theta(\tau + 1) &= \theta(\tau) + h\omega(\tau) \\ \omega(\tau + 1) &= \omega(\tau) + h\alpha(\theta(\tau), \omega(\tau), F(\tau)) \\ p(\tau + 1) &= p(\tau) + hv(\tau) \\ v(\tau + 1) &= v(\tau) + ha(\theta(\tau), \omega(\tau), F(\tau)). \end{aligned} \quad (18)$$

In this paper, the parameters of the cartpole example are given as follows. The sampling time is chosen as  $h = 0.02$ ; the mass of the cart, mass of the pole, gravitational acceleration, and half length of the pole are given by  $m_c = 1, m_p = 0.1, g = 9.8$  and  $\ell = 0.5$ . The objective function is also chosen as a typical linear quadratic form with the terminal state penalty:

$$J = x(T)^T Q_T x(T) + \sum_{\tau=0}^{T-1} \left( x(\tau)^T Q x(\tau) + u(\tau)^T R u(\tau) \right), \quad (19)$$

where the weighting matrices are chosen as  $Q = \text{diag}\{1, 0.1, 1, 1\}$  and  $R = 0.1$ ; the terminal weighting matrix is chosen as  $Q_T = \text{diag}\{10000, 1000, 0, 0\}$ . The initial state vector is chosen as  $x_0 = [\pi \ 0 \ 0 \ 0]^T$ , which means that the static pole is at the stable position .

The pretraining details are given as follows. The number of trials is chosen as 100, and the prediction horizon is chosen as 150. The initial state vector is chosen as  $x_0 = [\pi \ 0 \ 0 \ 0]^T$  at the time stamp  $\tau = 0$ . The force  $F$  is drawn from a uniform distribution within the range  $[-15, 15]$ .

### B. Neural Network Architecture and Pretraining Analysis

In this paper, we propose the use of three neural network structures and compare the performance attained by each of them. The first two types of the neural network structure are with three fully connected layers including two hidden layers and one output layer. In each hidden layer, a linear layer is followed by a batch normalization layer and a rectified linear unit (ReLU) layer, and the output layer is a simple fully connected linear layer. The layer size of the two fully connected neural network are given in Table I, where FCNN is short for fully connected neural network.

TABLE I  
LAYER SIZE FOR THE FULLY CONNECTED NEURAL NETWORK

Network	First Hidden Layer	Second Hidden Layer	Output Layer
Small FCNN	$[(m+n) \times 128]$	$[128 \times 64]$	$[64 \times n]$
Large FCNN	$[(m+n) \times 1024]$	$[1024 \times 512]$	$[512 \times n]$

Fig. 2 shows the third type of the neural network, which is basically a residual neural network (ResNet). A total of nine layers exist in this network, which comprise eight layers with shortcuts and one fully connected linear output layer.

To compare the training performance of each neural network, we perform the training for five times on the randomly generated dataset, with different seeds in terms of each network structure. Besides, we also generate the corresponding validation set and check the loss on the validation set during the training process. The dataset parameters are listed in



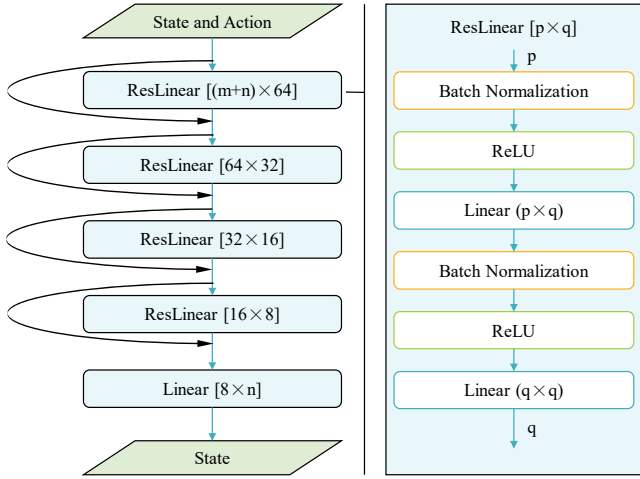


Fig. 2. Residual neural network architecture.

TABLE II  
PARAMETERS OF THE DATASET

Example	Dataset	Trials	Prediction Horizon	Dataset Size
Vehicle Tracking	Training	100	100	10000
	Validation	10	100	1000
Cartpole Swing-up	Training	100	150	15000
	Validation	10	150	1500

Table II. The training parameters are chosen as the same and listed as follows: The optimization algorithm is chosen as the Rectified Adam (RAdam); the linear rate is 0.001; the loss function is chosen as the mean squared error loss (MSELoss); the weight decay is  $1 \times 10^{-4}$ . Note that the training will be terminated when the loss value on the training set is less than  $1 \times 10^{-4}$ .

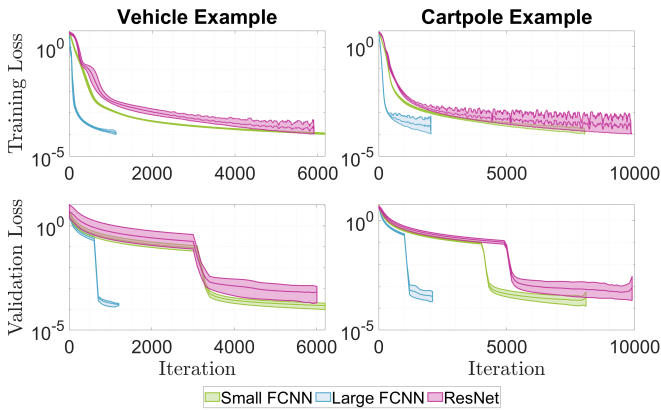


Fig. 3. Pretraining performance of different neural network architectures.

Fig. 3 shows the pretraining performance for different neural network architectures in terms of the loss value on the training set and validation set, respectively, and the time for the pretraining procedure is listed in Table III. For Fig. 3, the loss data is smoothed by performing average on every 500 data points. From both of the Fig. 3 and Table III, it shows that the large FCNN architecture usually demonstrates better

performance. Both the pretraining time and iteration number of the large FCNN are smaller than the other two architectures. In addition, in terms of the large FCNN architecture, the variation on the validation set is also smaller than the other two architectures.

TABLE III  
PRETRAINING TIME FOR DIFFERENT NEURAL NETWORK ARCHITECTURES

Example	Time (s)		
	Small FCNN	Large FCNN	ResNet
Vehicle Tracking	246.3256	121.0006	205.6572
Cartpole Swing-up	63.7257	28.1529	210.2348

## V. DISCUSSION ON THE NNILQR PERFORMANCE

In this section, the analysis on the NNILQR performance is presented and the influence of several critical factors in the NNILQR architecture is discussed. Note that these factors include the neural networks structure, the standard deviation parameter in the Gaussian filter, and the parameter in the exploration period.

### A. Effectiveness of the NNILQR Method

To demonstrate the effectiveness of the NNILQR method, we use the classical iLQR method as the benchmark and compare the NNILQR method to the classical iLQR method. The NNILQR method is randomly performed for five times with each neural network structure, and the classical iLQR method is performed with the same parameters as used in the NNILQR method.

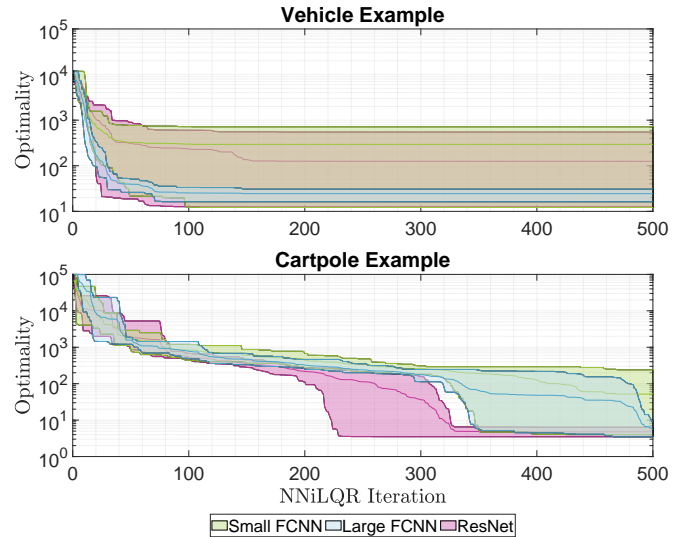


Fig. 4. Objective function value of the NNILQR method in different iterations.

Fig. 4 shows the optimality of the NNILQR method with respect to different neural network structures after 500 NNILQR iterations, where one NNILQR iteration includes one backward pass and one forward pass exactly; the optimality denotes the difference between the objective function values obtained by

the NNiLQR method during iterations and the optimal objective function value derived by the classical iLQR method given the dynamic model. The optimal objective function values derived by the classical iLQR method in the vehicle and cartpole examples are given by  $4.50320 \times 10^3$  and  $1.14152 \times 10^3$ , respectively. From Fig. 4, it can be seen that the NNiLQR method with all the three neural network structures can find a feasible solution with satisfying performance (in terms of the objective function value). It also shows that different neural network structures can lead to different performance. The large FCNN structure shows the highest performance in the vehicle tracking example but the ResNet structure demonstrates the best performance in the cartpole swing-up example. Basically, both the large FCNN structure and ResNet structure provide satisfying results and show higher performance than the small FCNN structure.

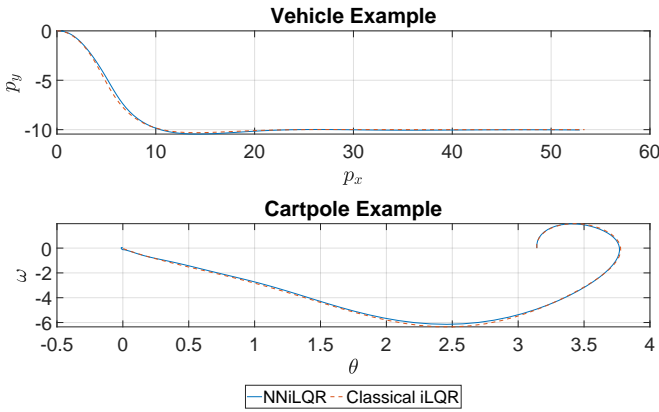


Fig. 5. Optimal trajectory obtained by the classical iLQR and NNiLQR method.

Fig. 5 shows the optimal trajectories obtained by the NNiLQR method with the large FCNN structure and the classical iLQR method. It indicates that in both examples, the trajectory derived by the NNiLQR method is almost the same as the trajectory derived by the classical iLQR method, and this also validates the effectiveness of the NNiLQR method.

### B. Influence of the Gaussian Filter

In this section, the performance of the NNiLQR method with different standard deviation parameter in the Gaussian filter is compared. Fig. 6 shows the optimality of the NNiLQR method with different standard deviation parameter in the Gaussian filter. From Fig. 6, it shows that the incorporation of the Gaussian filter improves the convergence and the optimality of the obtained trajectory. However, too large standard deviation parameter can suppress the useful information and impedes finding the optimal trajectory. The experiments in the two examples show that it is usually rational to choose the standard deviation from 1 to 10.

Fig. 6 shows the action sequences obtained by the NNiLQR method with different standard deviation parameters in the Gaussian filter. The smoothness of the action sequences in both examples is significantly improved with the larger standard deviation parameter in the Gaussian filter. However, too large

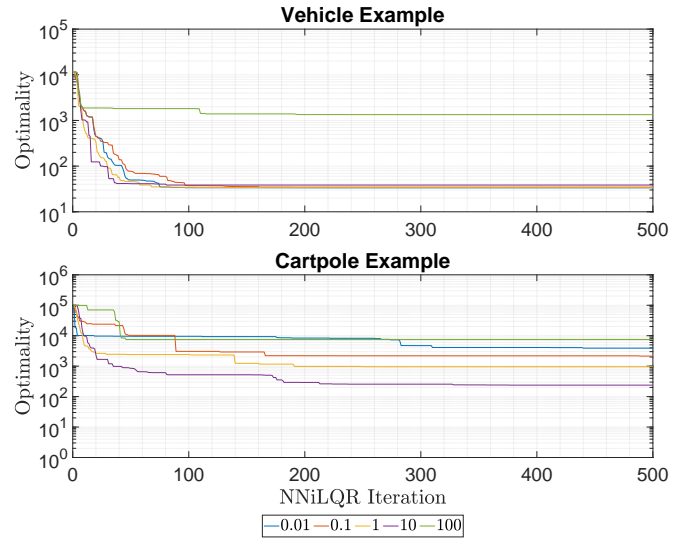


Fig. 6. Optimality of the NNiLQR method with different standard deviation parameters in the Gaussian filter in different iterations.

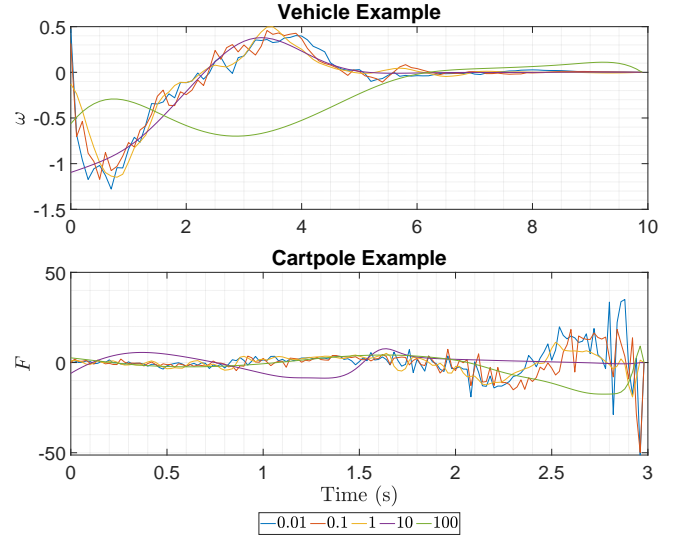


Fig. 7. Action sequence obtained by the NNiLQR method with different standard deviation parameters in the Gaussian filter.

standard deviation parameter also leads to too smooth action sequences such that the optimality cannot be ensured. From Fig. 6, it also shows that the reasonable range of the standard deviation parameter is from 1 to 10.

### C. Influence of the Number of Trials

Fig. 8 shows the optimality of the NNiLQR method with different number of trials. From Fig. 8, it shows that the larger number of trials usually improves the convergence and the optimality of the obtained trajectory. However, too large number of trials can lead to the difficulty in training the neural network. The experiments in the two examples show that it is usually rational to choose the number of trials to be around 100.

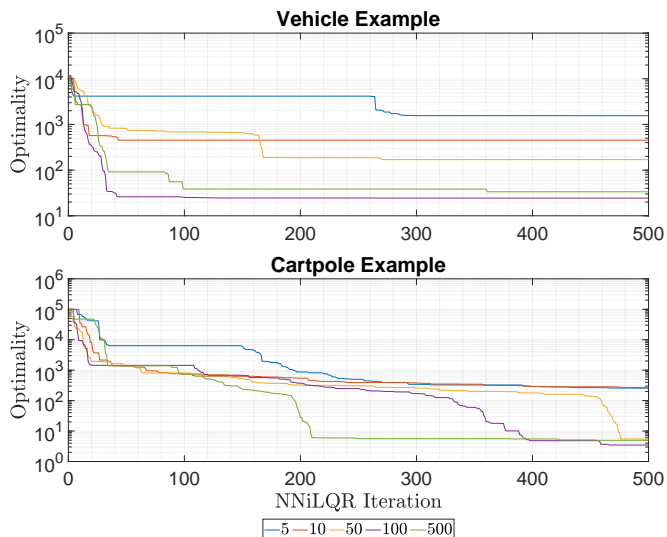


Fig. 8. Optimality of the NNiLQR method with different number of trials during the pretraining period in different iterations.

#### D. NNiLQR Performance with the Worse Pretraining Set

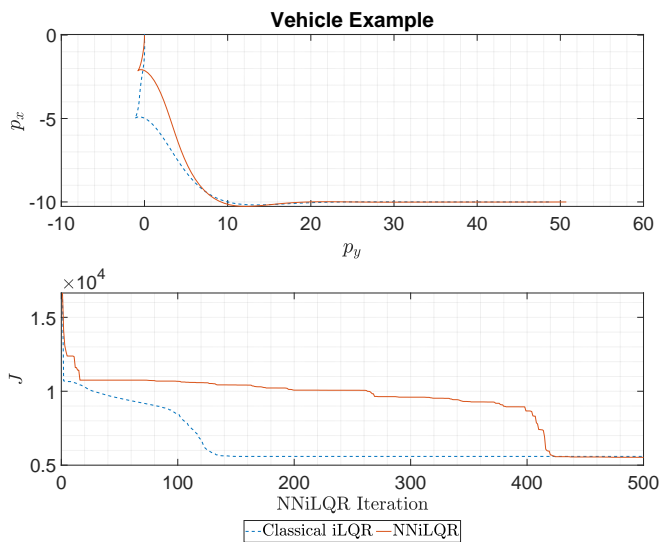


Fig. 9. Objective function value of the classical iLQR and NNiLQR method in different iterations.

To demonstrate the NNiLQR performance with the worse pretraining set, we set the initial state vector as  $x_0 = [0 \ 0 \ \pi/2 \ 0]^T$ , which means that initially, the vehicle heads towards the positive direction of the y-axis. In this case, the best strategy to minimize the objective function value is to reverse the car for a short distance and then go forward, as is shown in the first sub-figure of Fig. 9. During the pretraining period, we only consider the case where the vehicle goes forward. Therefore, in order to explore the performance with the reversing operation, it is necessary to perform the further exploration.

The first sub-figure in Fig. 9 shows the trajectories obtained by the classical iLQR method and the NNiLQR method. It is obvious that both trajectories successfully realize the

optimization objective of tracking. The second sub-figure in Fig. 9 shows the objective function value in the different iterations. From Fig. 9, it shows that the classical iLQR method can converge faster since it can employ the prior information from the dynamic model. However, the objective function value of the NNiLQR method is reduced at the very beginning utilizing the information of the pretraining, and then stuck at a large value for a long time to do the further exploration. It finally converge to the optimal trajectory based on the information from the further exploration.

Notably, the optimal objective function value obtained by the classical iLQR method is 5592.4 and the optimal objective function value obtained by the NNiLQR method is 5534.6 which means the performance of the trajectory obtained by the NNiLQR method is indeed slightly better than the classical iLQR method. This is because the further exploration is implemented in the NNiLQR method such that it will not be stuck at the local optimal point.

#### E. Python iLQR Solver Package

In this paper, all the experiments are implemented on a desktop with the CPU Intel(R) Xeon(R) CPU E5-2695 v3 @ 2.30GHz and the GPU RTX2080. All the simulation results are obtained based on the Python iLQR solver package developed by the team of the authors, and the package is completely open-source and available with the Github link as follows: <https://github.com/cheng-zilong/PyiLQR.git>.

In the developed iLQR solver package, the basic iLQR method is accelerated by the open source just-in-time (JIT) compiler package Numba. Therefore, the fundamental iLQR iterations can be implemented with extremely high efficiency, which facilitates the use in real-time applications without any difficulty. The integrated neural network system in the developed package is supported by the Python deep learning package Pytorch, which is accelerated by the CUDA toolkit.

## VI. CONCLUSION

This paper investigates the development of the NNiLQR method, a reinforcement learning architecture. In view of an unknown dynamic system, a neural network is utilized to fit the dynamic function in an iterative framework, which enables the use of the iLQR method in trajectory planning problems. The estimated gradient matrix of the dynamic function is derived, and the improved feedforward iteration is proposed to deal with the inaccuracy and imprecision in the optimization problem. As a result, the refined iLQR method can be applied completely without any prior information of the dynamic system. Moreover, the trajectory resulted from the NNiLQR method can be even better than the classical iLQR method, as the local optimal point can be escaped with the deployment of the further exploration procedure. Finally, illustrative examples are used to validate the performance of the proposed NNiLQR method and detailed discussions are included. As illustrated from the examples, the significance as claimed in this work is suitably demonstrated. It is worthwhile to highlight that due to the effectiveness of this proposed NNiLQR approach, it suitably addresses the practical appeal in many real-world

applications, including but not limited to robotics, autonomous driving, computer vision, electronic games, etc.

## REFERENCES

- [1] R. Song, F. L. Lewis, and Q. Wei, "Off-policy integral reinforcement learning method to solve nonlinear continuous-time multiplayer nonzero-sum games," *IEEE Transactions on Neural Networks and Learning Systems*, vol. 28, no. 3, pp. 704–713, 2016.
- [2] B. Kiumarsi, K. G. Vamvoudakis, H. Modares, and F. L. Lewis, "Optimal and autonomous control using reinforcement learning: A survey," *IEEE Transactions on Neural Networks and Learning Systems*, vol. 29, no. 6, pp. 2042–2062, 2017.
- [3] A. V. Nair, V. Pong, M. Dalal, S. Bahl, S. Lin, and S. Levine, "Visual reinforcement learning with imagined goals," in *Advances in Neural Information Processing Systems*, 2018, pp. 9191–9200.
- [4] C. Yang, C. Chen, W. He, R. Cui, and Z. Li, "Robot learning system based on adaptive neural control and dynamic movement primitives," *IEEE Transactions on Neural Networks and Learning Systems*, vol. 30, no. 3, pp. 777–787, 2018.
- [5] S. Fujimoto, D. Meger, and D. Precup, "Off-policy deep reinforcement learning without exploration," in *International Conference on Machine Learning*, 2019, pp. 2052–2062.
- [6] Y. Keneshloo, T. Shi, N. Ramakrishnan, and C. K. Reddy, "Deep reinforcement learning for sequence-to-sequence models," *IEEE Transactions on Neural Networks and Learning Systems*, 2019.
- [7] I. Clavera, J. Rothfuss, J. Schulman, Y. Fujita, T. Asfour, and P. Abbeel, "Model-based reinforcement learning via meta-policy optimization," *arXiv preprint arXiv:1809.05214*, 2018.
- [8] M. Liu, Y. Wan, F. L. Lewis, and V. G. Lopez, "Adaptive optimal control for stochastic multiplayer differential games using on-policy and off-policy reinforcement learning," *IEEE Transactions on Neural Networks and Learning Systems*, 2020.
- [9] J.-H. Kim and F. L. Lewis, "Model-free  $H_\infty$  control design for unknown linear discrete-time systems via Q-learning with LMI," *Automatica*, vol. 46, no. 8, pp. 1320–1326, 2010.
- [10] W. Zhao, H. Liu, and F. L. Lewis, "Robust formation control for cooperative underactuated quadrotors via reinforcement learning," *IEEE Transactions on Neural Networks and Learning Systems*, 2020.
- [11] Y. Tassa, N. Mansard, and E. Todorov, "Control-limited differential dynamic programming," in *2014 IEEE International Conference on Robotics and Automation (ICRA)*. IEEE, 2014, pp. 1168–1175.
- [12] A. Pavlov, I. Shames, and C. Manzie, "Interior point differential dynamic programming," *arXiv preprint arXiv:2004.12710*, 2020.
- [13] J. Chen, W. Zhan, and M. Tomizuka, "Autonomous driving motion planning with constrained iterative LQR," *IEEE Transactions on Intelligent Vehicles*, vol. 4, no. 2, pp. 244–254, 2019.
- [14] J. Ma, Z. Cheng, X. Zhang, M. Tomizuka, and T. H. Lee, "Alternating direction method of multipliers for constrained iterative LQR in autonomous driving," *arXiv preprint arXiv:2011.00462*, 2020.
- [15] A. El-Fakdi, M. Carreras, and P. Ridao, "Towards direct policy search reinforcement learning for robot control," in *2006 IEEE/RSJ International Conference on Intelligent Robots and Systems*. IEEE, 2006, pp. 3178–3183.
- [16] C. Celemin, G. Maeda, J. Ruiz-del Solar, J. Peters, and J. Kober, "Reinforcement learning of motor skills using policy search and human corrective advice," *The International Journal of Robotics Research*, vol. 38, no. 14, pp. 1560–1580, 2019.
- [17] R. S. Sutton, "Dyna, an integrated architecture for learning, planning, and reacting," *ACM Sigart Bulletin*, vol. 2, no. 4, pp. 160–163, 1991.
- [18] W. Montgomery, A. Ajay, C. Finn, P. Abbeel, and S. Levine, "Reset-free guided policy search: Efficient deep reinforcement learning with stochastic initial states," in *2017 IEEE International Conference on Robotics and Automation (ICRA)*. IEEE, 2017, pp. 3373–3380.
- [19] A. Yahya, A. Li, M. Kalakrishnan, Y. Chebotar, and S. Levine, "Collective robot reinforcement learning with distributed asynchronous guided policy search," in *2017 IEEE/RSJ International Conference on Intelligent Robots and Systems*. IEEE, 2017, pp. 79–86.
- [20] F. Renda, M. Giorelli, M. Calisti, M. Cianchetti, and C. Laschi, "Dynamic model of a multibending soft robot arm driven by cables," *IEEE Transactions on Robotics*, vol. 30, no. 5, pp. 1109–1122, 2014.
- [21] W. He, W. Ge, Y. Li, Y.-J. Liu, C. Yang, and C. Sun, "Model identification and control design for a humanoid robot," *IEEE Transactions on Systems, Man, and Cybernetics: Systems*, vol. 47, no. 1, pp. 45–57, 2016.
- [22] R. Buchanan, T. Bandyopadhyay, M. Bjelonic, L. Wellhausen, M. Hutter, and N. Kottege, "Walking posture adaptation for legged robot navigation in confined spaces," *IEEE Robotics and Automation Letters*, vol. 4, no. 2, pp. 2148–2155, 2019.
- [23] J. Ma, Z. Cheng, X. Zhang, A. A. Mamun, C. W. de Silva, and T. H. Lee, "Data-driven predictive control for multi-agent decision making with chance constraints," *arXiv preprint arXiv:2011.03213*, 2020.
- [24] D. Silver, R. S. Sutton, and M. Müller, "Reinforcement learning of local shape in the game of go," in *International Joint Conferences on Artificial Intelligence (IJCAI)*, vol. 7, 2007, pp. 1053–1058.
- [25] N. Ding and R. Soricut, "Cold-start reinforcement learning with softmax policy gradient," in *Advances in Neural Information Processing Systems*, 2017, pp. 2817–2826.
- [26] S. Khadka and K. Tumer, "Evolution-guided policy gradient in reinforcement learning," in *Advances in Neural Information Processing Systems*, 2018, pp. 1188–1200.
- [27] S. Li, Y. Wu, X. Cui, H. Dong, F. Fang, and S. Russell, "Robust multi-agent reinforcement learning via minimax deep deterministic policy gradient," in *Proceedings of the AAAI Conference on Artificial Intelligence*, vol. 33, 2019, pp. 4213–4220.
- [28] S. Gu, T. Lillicrap, I. Sutskever, and S. Levine, "Continuous deep Q-learning with model-based acceleration," in *International Conference on Machine Learning*, 2016, pp. 2829–2838.
- [29] T. Hester, M. Vecerik, O. Pietquin, M. Lanctot, T. Schaul, B. Piot, D. Horgan, J. Quan, A. Sendonaris, G. Dulac-Arnold *et al.*, "Deep Q-learning from demonstrations," *arXiv preprint arXiv:1704.03732*, 2017.
- [30] X. Dong, J. Shen, W. Wang, Y. Liu, L. Shao, and F. Porikli, "Hyperparameter optimization for tracking with continuous deep Q-learning," in *Proceedings of the IEEE Conference on Computer Vision and Pattern Recognition*, 2018, pp. 518–527.
- [31] F. Moreno-Vera, "Performing deep recurrent double Q-learning for atari games," in *2019 IEEE Latin American Conference on Computational Intelligence (LA-CCI)*. IEEE, 2019, pp. 1–4.
- [32] V. R. Konda and J. N. Tsitsiklis, "Actor-critic algorithms," in *Advances in Neural Information Processing Systems*, 2000, pp. 1008–1014.
- [33] V. Mnih, A. P. Badia, M. Mirza, A. Graves, T. Lillicrap, T. Harley, D. Silver, and K. Kavukcuoglu, "Asynchronous methods for deep reinforcement learning," in *International Conference on Machine Learning*, 2016, pp. 1928–1937.
- [34] R. Lowe, Y. I. Wu, A. Tamar, J. Harb, O. Pieter Abbeel, and I. Mordatch, "Multi-agent actor-critic for mixed cooperative-competitive environments," *Advances in Neural Information Processing Systems*, vol. 30, pp. 6379–6390, 2017.
- [35] H. Kumar, A. Koppel, and A. Ribeiro, "On the sample complexity of actor-critic method for reinforcement learning with function approximation," *arXiv preprint arXiv:1910.08412*, 2019.
- [36] Q. Wei, L. Wang, Y. Liu, and M. M. Polycarpou, "Optimal elevator group control via deep asynchronous actor-critic learning," *IEEE Transactions on Neural Networks and Learning Systems*, 2020.
- [37] D. Mitrovic, S. Klanke, and S. Vijayakumar, "Adaptive optimal feedback control with learned internal dynamics models," in *From Motor Learning to Interaction Learning in Robots*. Berlin: Springer, 2010, vol. 264, pp. 65–84.
- [38] S. Levine and V. Koltun, "Guided policy search," in *International Conference on Machine Learning*, 2013, pp. 1–9.
- [39] Y. Pan and E. Theodorou, "Probabilistic differential dynamic programming," in *Advances in Neural Information Processing Systems*, 2014, pp. 1907–1915.
- [40] A. Yamaguchi and C. G. Atkeson, "Differential dynamic programming with temporally decomposed dynamics," in *2015 IEEE-RAS 15th International Conference on Humanoid Robots (Humanoids)*. IEEE, 2015, pp. 696–703.
- [41] —, "Neural networks and differential dynamic programming for reinforcement learning problems," in *2016 IEEE International Conference on Robotics and Automation (ICRA)*. IEEE, 2016, pp. 5434–5441.
- [42] J. Viereck, J. Kozolinsky, A. Herzog, and L. Righetti, "Learning a structured neural network policy for a hopping task," *IEEE Robotics and Automation Letters*, vol. 3, no. 4, pp. 4092–4099, 2018.
- [43] S. Bechtel, Y. Lin, A. Rai, L. Righetti, and F. Meier, "Curious iLQR: Resolving uncertainty in model-based RL," in *Conference on Robot Learning*. PMLR, 2020, pp. 162–171.
- [44] A. Nagariya and S. Saripalli, "An iterative LQR controller for off-road and on-road vehicles using a neural network dynamics model," *arXiv preprint arXiv:2007.14492*, 2020.
- [45] K. S. Parunandi, A. Sharma, S. Chakravorty, and D. Kalathil, "D2C 2.0: Decoupled data-based approach for learning to control stochastic non-

linear systems via model-free iLQR,” *arXiv preprint arXiv:2002.07368*, 2020.

- [46] Y. Tassa, T. Erez, and E. Todorov, “Synthesis and stabilization of complex behaviors through online trajectory optimization,” in *2012 IEEE/RSJ International Conference on Intelligent Robots and Systems*. IEEE, 2012, pp. 4906–4913.
- [47] Y. Pan, G. I. Boutselis, and E. A. Theodorou, “Efficient reinforcement learning via probabilistic trajectory optimization,” *IEEE Transactions on Neural Networks and Learning Systems*, vol. 29, no. 11, pp. 5459–5474, 2018.